Published online 4 October 2013 *Nucleic Acids Research, 2014, Vol. 42, No. 1* ***553–566***
doi:10.1093/nar/gkt889

Handling the 3-methylcytosine lesion by six human DNA polymerases members of the B-, X- and Y-families

Antonia Furrer and Barbara van Loon*

Institute of Veterinary Biochemistry and Molecular Biology, University of Zürich, Winterthurerstrasse 190, 8057 Zürich, Switzerland

Received July 2, 2013; Revised August 26, 2013; Accepted September 10, 2013

ABSTRACT

Alkylating agents often generate 3-methylcytosine (3meC) lesions that are efficiently repaired by AlkB homologues. If AlkB homologue proteins are not functional, or the number of 3meC lesions exceeds the cellular repair capacity, the damage will persist in the genome and become substrate of DNA polymerases (Pols). Though alkylating agents are present in our environment and used in the clinics, currently nothing is known about the impact of 3meC on the accuracy and efficiency of human Pols. Here we compared the 3meC bypass properties of six human Pols belonging to the three families: B (Pol δ), X (Pols β and λ) and Y (Pols κ, ι and η). We show that under replicative conditions 3meC impairs B-family, blocks X-family, but not Y-family Pols, in particular Pols η and ι. These Pols successfully synthesize opposite 3meC; Pol ι preferentially misincorporates dTTP and Pol η dATP. The most efficient extenders from 3meC base-paired primers are Pols κ and η. Finally, using xeroderma pigmentosum variant patient cell extracts, we provide evidence that the presence of functional Pol η is mandatory to efficiently overcome 3meC by mediating complete bypass or extension. Our data suggest that Pol η is crucial for efficient 3meC bypass.

INTRODUCTION

Living organisms are exposed to alkylating agents present in shape of endogenous sources, such as cellular metabolism, exogenously in the environment, and in clinics as one of the most frequently used cancer chemotherapeutic drugs (1,2). Exposure of genomic DNA to alkylating agents often results in cytotoxic and/or carcinogenic mutations (3). Consequently, alkylation chemotherapy was shown to potentially induce secondary cancers characterized by genome instability and mutation accumulation (4). Alkylation DNA lesions, induced by S_N2 alkylating agents, include 3-methylcytosine (3meC), 3-methylthymine, 1-methyladenine and 1-methylguanine (5). 3meC lesions are predominantly generated in single-stranded (ss) DNA during replication, repair and transcription. In double-stranded (ds) DNA, the reactive site is involved in base pairing and thus protected from modification (6). The 3meC lesions are efficiently repaired via direct oxidative reversal, mediated by iron(II) and 2ketoglutarate (2KG)dependent dioxygenases: alkylation protein B (AlkB) in prokaryotes (7) and the AlkB homologues (ALKBH) 2 and 3 in eukaryotes (8,9). AlkB deficient *Escherichia coli* cells have elevated amount of alkylated lesions, display increased mutation frequency and are hypersensitive to alkylating agents (10,11). Similarly, exposure of mammalian cells lacking ALKBH2 to the alkylating agent methylmethane sulfonate (MMS) results in increased cytotoxicity and mutagenicity (12,13). Compared with ALKBH2 proficient, the deficient cells are characterized with large increase in C→A and to certain extent C→T mutations, when treated with MMS (13). Additionally, ALKBH2 has been implicated in cancerogenesis, by influencing cancer progression, as well as sensitivity to cisplatin treatment (14,15). Efficient removal of alkylation DNA damage is thus critical for cellular function, preservation of genomic integrity and survival.

Increased cytotoxicity and mutation frequency, due to loss of functional AlkB or ALKBH2, suggest an impaired action of DNA polymerases (Pols) at the site of unrepaired alkylation damage. Besides a malfunctional direct reversal pathway, Pols can face 3meC in case: (i) when the amount of DNA damage exceeds the cellular repair capacity as well as (ii) if alkylation damage of

*To whom correspondence should be addressed. Tel: +41 44 635 54 67; Fax: +41 44 635 68 40; Email: bvanloon@vetbio.uzh.ch

ssDNA occurs during DNA replication or repair. Upon encountering the DNA lesion, Pols can either (i) be completely blocked, (ii) incorporate a nucleotide opposite the damage and then be blocked due to inability to extend or (iii) fully bypass by base pairing and extending past the lesion. Understanding the role(s) of the different Pols in the bypass of alkylation damage is complicated by the number of different Pols present in every organism, with a broad range of catalytic properties. For example, the prokaryotic organism *E. coli* contains five different Pols (16), whereas in eukaryotes sixteen Pols have been identified and, based on the sequence homology, grouped in five families—A, B, X, Y and reverse transcriptase (17). Addition of a methyl group to endocyclic N-atoms and subsequent generation of 3meC, 3-methylthymine, 1-methyladenine and 1-methylguanine lesions leads to DNA replication block in *E. coli*, potentially due to impairment of B-family replicative Pol III (10). In addition, the *E. coli* A-family gap-filling Pol I is inhibited by 3meC damage and besides certain incorporation of dGTP, it can misincorporate dATP and dTTP opposite the lesion (18,19). While the replicative Pols are characterized with a high fidelity enabled by a tight-fitting active site and 3′→5′ proofreading activity, the active sites of X- and Y-family translesion synthesis (TLS) Pols, which also lack a 3′→5′ proofreading exonuclease activity, can readily accommodate and efficiently bypass different DNA damages. At the same time, this results in an increased error-rate on undamaged DNA (20–22). Accumulation of the Y-family TLS Pols, as result of SOS-response activation in *E. coli*, increases bypass efficiency of the 3-methylpirimidine and 1-methylpurine lesions by 3–4-fold (10,11). A recent structural study provided valuable insight into the features of prokaryotic Y-family Dpo4-mediated bypass of 3meC lesion (23). Presence of 3meC results in inhibition of Dpo4 and generation of ∼60% mutagenic products during remaining bypass (23). Crystal structure of Dpo4 ternary extension complex with correct and mismatched 3′-terminal primer base opposite the 3meC lesion indicates that the lesion remains positioned within the DNA template/primer helix, whereas the correct as well as incorrect nucleotides paired to 3meC are misaligned and exhibit significant primer terminal distortion (23). Unfortunately, similar structural or mechanistic studies in the presence of the blocking and mutagenic 3meC lesion with eukaryotic Pols are currently lacking.

In this work, we characterized the impact of the 3meC lesion on six human Pols belonging to the three families B (Pol δ), X (Pols β and λ) and Y (Pols κ, ι and η). The properties of human Pols were compared on (i) running- and standing-start templates mimicking replicative conditions, as well as (ii) 29-, 7- and 1-nucleotide (nt) gap constructs resembling nucleotide excision (NER) and base excision repair (BER) intermediates, respectively. By using recombinant proteins, we show that under replicative conditions, 3meC impairs human B-family, represents a block for X-family enzymes, but can be successfully utilized by Y-family Pols, especially Pols ι and η. Single nucleotide incorporation experiments reveal that Pols ι and η successfully base-pair 3meC, Pol ι by preferentially misincorporating dTTP and Pol η dATP. The most efficient extenders of base-paired 3meC are Pols κ and η, their activity depending on the DNA structure. Finally, by using human cell extracts, we provide evidence that in the context of the cell the Pol crucial for efficient 3meC bypass is Pol η, as its lack results in an inability to successfully overcome the lesion. These results suggest the existence of a novel Pol η-dependent pathway that could reduce the mutagenic effects of alkylation treatment and potentially facilitate cellular survival, especially under conditions when the functional ALKBH proteins, responsible for direct reversal repair, are missing.

MATERIALS AND METHODS

Labeled γ[^{32}P] ATP was purchased from Hartmann Analytic. Deoxyribonucleoside triphosphates were from Sigma. All other reagents were of analytic grade and purchased from Fluka, Sigma or Merck. The 40, 39, 35, 32, 26 and 17mer and oligonucleotides were obtained from Microsynth, whereas 72mer containing 3meC lesion or undamaged C were purchased were from Purimex.

Preparation of DNA substrates

The sequences of the oligonucleotides used were as follows: 72mer template, 5′GTATTAGATATTCGGGAGGTTGGGCGCCGGCGXTGTGAATTCGGCACTGGCCGTCGTATGCTCTTGGTTGTA3′; 40mer primer, 5′TACAACCAAGAGCATACGACGGCCAGTGCCGAATTCACAN3′; 39mer primer, 5′TACAACCAAGAGCATACGACGGCCAGTGCCGAATTCACA3′; 17mer primer, 5′TACAACCAAGAGCATAC3′; 35mer 5′AAAAAAAAAAAAAAAAAAAAAAAAAAAAAAAAA3′; 32mer 5′CGCCGGCGCCCAACCTCCCGAATATCTAATAC3′; and 26mer, 5′CGCCCAACCTCCCGAATATCTAATAC3′. The letter X corresponds to the position of 3meC and C in the damaged and undamaged DNA template, respectively. The letter N in 40mer indicates four possible nucleotides at the primer 3′ terminus: G, A, T or C. These four different 40mers were annealed to template strand and used in the extension assay experiments (Figure 5 and Supplementary Figure S6). The primer/template resembling running-start conditions was generated by annealing 17mer primer and 72mer template (Figure 1 and Supplementary Figure S1), whereas annealing of 39mer primer and the same template resulted in standing-start situation (Figures 2, 6 and Supplementary Figure S2). The 29-nt gap construct was created by annealing 17mer primer and 26mer downstream oligonucleotide to 72mer template (Figure 3 and Supplementary Figure S3). Annealing of 39mer primer and downstream 32mer to 72mer template yielded 1-nt gap construct (Figure 4). When instead of 32mer a 26mer was used, 7-nt gap was generated (Supplementary Figures S4 and S5).

The 17, 39 and 40mer primers were labeled with T4 polynucleotide kinase (New England Biolabs) in the presence of [^{32}P] ATP. Each labeled oligonucleotide was mixed with the 72mer template oligonucletide at 1:1 (M/M) ratio in the presence of 20 mM Tris–HCl (pH 7.4) and 150 mM NaCl, heated at 95°C for 10 min

and then slowly cooled down at room temperature. Similarly, to obtain 29-, 7- and 1-nt gap constructs, labeled primer, template and downstream oligonucleotide were mixed in ration 1:1:1 (M/M/M).

Expression and purification of recombinant proteins

Human recombinant Pol δ and PCNA were expressed and purified as described in (24,25). Human recombinant Pols λ and β were purified as noted previously in (26). The bacterial clones for the expression of human Pols η and ι were a gift from Roger Woodgate (NIH, USA). Human recombinant Pols η and ι were expressed and purified as described (27). Pol κ was purchased from Enzymax, USA.

Cell lines and culture conditions

XP30R0 fibroblasts are simian virus 40-transformed cells derived from a patient suffering from the variant form of xeroderma pigmentosum (XPV). The cells harbor a 13-bp deletion resulting in the expression of a truncated and non-functional Pol η. XP30R0 cell line was a gift from Alan Lehman (University of Sussex, Brighton, UK). Cells were grown in a humidified 5% CO2 atmosphere in Dulbecco's modified Eagle's medium containing GlutaMAX-I supplemented with 10% fetal bovine serum and 100 U/ml penicillin–streptomycin (all obtained from Gibco, Invitrogen). To overexpress human Pols η and ι mammalian expression vectors pJRM56 and pJRM46 [provided by Roger Woodgate (NIH, USA)] were used. Empty vector pcDNA 3.1 (Invitrogen), pJRM46 or pJRM56 expression constructs were transiently transfected into XPV cells using lipofectamine (Invitrogen) according to manufacturers protocol. Forty-eight hours after the transfection, cells were harvested and whole-cell extract (WCE) prepared.

Preparation of WCE

Cells were trypsinized, washed twice with cold PBS and resuspended in three packed cell volumes of hypotonic lysis buffer [10 mM Tris–HCl (pH 8), 1 mM EDTA, 10%(w/v) sucrose, 10% (v/v) glycerol, 0.1 mM PMSF, 1 mM DTT, 1 μg/ml pepstatine, 1 μg/ml bestatine and 1 μg/ml leupeptin]. After swelling for 20 min at 4°C, cells were lysed with a Dounce homogenizer (tight pastille). NaCl was added next to a final concentration 0.35 M and incubated 10 min at 4°C. Samples were diluted with seven packed cell volumes of lysis buffer, sonicated and centrifuged 20 min at 15 000 *g*. The supernatants were flash frozen in liquid N_2 or analyzed directly.

Protein analysis

WCEs were separated on 10% Bis-Tris poly-acrylamide gels followed by transfer to Immobilon-FL membrane (Millipore) for immunoblotting analysis. Primary antibodies against Pol η (Abcam), Pol ι [custom made antibody, provided by Roger Woodgate (NIH, USA)] and Tubulin (Sigma) were detected using infrared Dye-conjugated secondary antibodies (LI-COR Biosciences). The signal was visualized using direct infrared fluorescence via the Odyssey Scanner (LI-COR Biosciences).

Enzymatic assays

Recombinant human enzyme assays

For denaturing gel analysis of DNA synthesis products, the reaction mixture (10 μl) contained 40 mM Tris–HCl (pH 8), 10 mM DTT and 250 μg/ml bovine serum albumin. In case of Pol δ reactions, 5 mM Mg^{2+} was present, whereas for all other Pols, 1 mM Mg^{2+} was used. Concentrations of Pols and the 5′ ^{32}P-labeled DNA in the reaction were as indicated in the Figures, as well as Figure Legends. The amounts of dNTPs were as follows: 10 μM for Pol δ, 1 μM in case of Pol λ and 5 μM for all other Pols. All reactions were performed at 37°C for 15 min, and the reaction products analyzed by 7 M urea/12.5% polyacrylamide gel electrophoresis.

Assay with WCEs

For denaturing gel analysis of DNA synthesis products, the 10 μl of reactions containing 40 mM Tris–HCl (pH 8), 10 mM DTT and 250 μg/ml bovine serum albumin, 1 mM Mg^{2+}, 2 nM 5′ ^{32}P-labeled DNA, 10 μM unlabeled 35mer trap DNA, 100 μM dNTPs and 3 μl of (1.33 μg/μl) WCE were incubated at 37°C for 30 min, and reaction products were separated by 7 M urea/12.5% polyacrylamide gel electrophoresis.

Steady state kinetic analysis

Reactions were performed as described earlier in the text, each reaction containing 20 nM of DNA template and 15 nM of either Pol ι or η. Quantification was performed by densitometry with a PhosphorImager (Typhoon Trio, GE Healthcare). The initial velocities of the reaction were calculated from the values of integrated gel band intensities with the programs GelEval 1.35 scientific imaging software (FrogDance Software, UK) and GraphPad Prism 5.0:

$$I^*T/IT - 1,$$

where T is the target site, the template position of interest; I^*T is the sum of the integrated intensities at positions T, $T+1,\ldots, T+n$. All of the intensity values were normalized to the total intensity of the corresponding lane to correct for differences in gel loading. The apparent k_M and k_{cat} values were calculated by plotting the initial velocities in dependence of the nucleotide [dNTP] or primer [3′-OH] substrate concentrations and fitting the data according to Michaelis–Menten equation:

$$k_{cat}[E]_0/(1 + k_M/[S]),$$

where $[E]_0$, was the input enzyme concentration and $[S]$ was the variable substrate. Substrate incorporation efficiencies were defined as the k_{cat}/k_M ratio. Under single nucleotide incorporation conditions, $kcat = k_{pol}k_{off}/(k_{pol} + k_{off})$ and $k_M = k_d k_{off}/(k_{pol} + k_{off})$, with k_{pol} being the true polymerization rate, k_{off} the dissociation rate of the enzyme–primer complex and k_d the true Michelis constant for nucleotide binding. Thus, k_{cat}/k_M values are equal to k_{pol}/k_d. Substrate concentrations used for dNTPs were 0.1–10 μM.

Time-dependent accumulation of products was fitted to the mixed exponential equation:

$$[P] = A(1 - e^{-k_{obs}t}) + k_{ss}t,$$

where $[P]$ designates the products formed, A the burst amplitude, t time, k_{obs} the apparent burst rate, and k_{ss} the steady-state rate, which corresponds to k_{off}.

Free energy change ($\Delta\Delta G$) values were estimated according to the relationship:

$$\Delta\Delta G = R\mathrm{T}\ln(k),$$

where R is the gas constant ($1.9872\,\mathrm{cal} \times \mathrm{mol}^{-1} \times \mathrm{K}^{-1}$), T is the absolute temperature (K), and k is the ratio between the kinetic constants considered.

RESULTS

The Y-family DNA polymerase η successfully bypasses 3meC

3meC is predominantly generated in ssDNA, which is largely present during DNA replication. To address the impact of 3meC damage occurring directly in front of the replication machinery, bypass efficiency of six human Pols was tested under running-start conditions (Figure 1A), using a primer/template containing the lesion at position +23 from the primer. For efficient lesion bypass, Pols need to elongate the primer up to the lesion, incorporate a nucleotide opposite the damage and extend from it. The activity of the major lagging-strand replicative Pol δ was partially impaired in the presence of 3meC damage (Figure 1B). Pol δ reached the lesion and incorporated a nucleotide opposite 3meC; however, its further extension was reduced resulting in very limited amount of full-length product (Figure 1B, lanes 2–4). This suggested that, upon encountering the lesion, the replication fork could potentially be significantly slowed-down or stalled and for its successful continuation another more specialized Pol would be required. The repair X-family Pols β and λ are known to bypass small base lesions (17,20), but they were fully blocked by the 3meC damage (Figure 1B, lanes 6–12). The three different members of TLS Y-family Pols κ, ι and η were tested next on 3meC (Figure 1C). As a template DNA in its sequence contains all four bases including undamaged T, which Pol ι favorably mispairs with 'wooble' G (28), Pol ι was unable to efficiently elongate the running-start primer and reach the lesion (Figure 1C, lanes 6–8). Pol κ in contrast very efficiently elongated the primer, but exhibited strong pausing at the position immediately preceding the lesion. It nonetheless was able to partially bypass 3meC, by generating products one or two nucleotides shorter than the full-length (Figure 1C, lanes 2–4). This suggested that Pol κ either loops out 3meC lesion and continues the synthesis or generates deletions during elongation after pairing of 3meC. To distinguish between the two, the length of Pol κ products was compared in the presence of undamaged and damaged running-start templates (Supplementary Figure S1A). In both cases, the products generated by Pol κ were one or two nucleotides shorter than the full-length (Supplementary Figure S1B, compare lanes 1–8 with lanes 9 and 10), thus indicating that under tested conditions, Pol κ most likely induces deletions during elongation. Pol η finally was the most efficient in bypassing 3meC under running-start conditions. Pol η in fact elongated the primer and efficiently generated full-length product, showing only a modest pausing at the lesion site (Figure 1C, lanes 11 and 12). Taken together, these first results indicated that under running-start conditions, 3meC (i) blocks human X-family Pols, (ii) impairs the activity of B-family Pol δ and Y-family Pol κ, but (iii) can successfully be processed by TLS Pol η.

DNA polymerases ι and η efficiently, but inaccurately, base-pair 3meC

While considering the bypass efficiency of a certain DNA lesion, it is additionally essential to determine its impact on Pol fidelity. To assess the accuracy of 3meC bypass, the primer was annealed to template strand directly in front of the lesion resulting in standing-start conditions (Figure 2A). The amount of dNTPs in the reaction was modulated according to the known affinity of each Pol. Replicative Pol δ under standing-start conditions preferentially misincorporated dATP, followed by dTTP opposite 3meC (Figure 2B, lanes 4 and 5). Additionally, in the presence of all 4 dNTPs, Pol δ incorporated a single nucleotide opposite the lesion and in comparison with control template exhibited dramatically reduced extension capacity (Figure 2B, lane 2; Supplementary Figure S2), thus confirming the observation from Figure 1B. The presence of 3meC on standing-start primer/template strongly inhibited the activity of Pols β and λ, as well as κ (Figure 2C–E). Interestingly, Pol κ weakly inserted two dCTPs (Figure 2E, lane 6), suggesting that under standing-start conditions, this Pol either (i) potentially skips 3meC and copies the next template base (G) twice or (ii) incorporates first dCTP opposite the lesion and the second one across subsequent template base. In comparison with other human Pols tested, the Y-family Pols ι and η efficiently base paired the lesion (Figure 2F and G). Interestingly, Pol ι more efficiently incorporated dGTP opposite 3meC, than across undamaged C (Figure 2F, compare lane 1 with lane 3). While Pol ι successfully mispaired 3meC with dTTP, Pol η with comparable efficiency incorporated the inaccurate dATP as well as the correct dGTP opposite 3meC (Figure 2F and G; Table 1). In addition, it also showed a low discrimination against the incorporation of dTTP and dCTP (Table 1). Similar to Pol κ, in the presence of dCTP incorporation of two nucleotides was observed (Figure 2G, lane 6). Suggesting that Pol η after copying the lesion incorporates second dCTP opposite the next template base or that it skips 3meC and copies subsequent template G twice. Overall, the substrate affinity and conversion efficiency were several fold higher for Pol η than ι (Table 1). Pol η further completed the bypass by generating full-length products in the presence of all 4 dNTPs (Figure 2G, lane 2). These findings suggested that Y-family Pols ι and η efficiently misincorporate nucleotides opposite 3meC, with Pol η being the more accurate of the two.

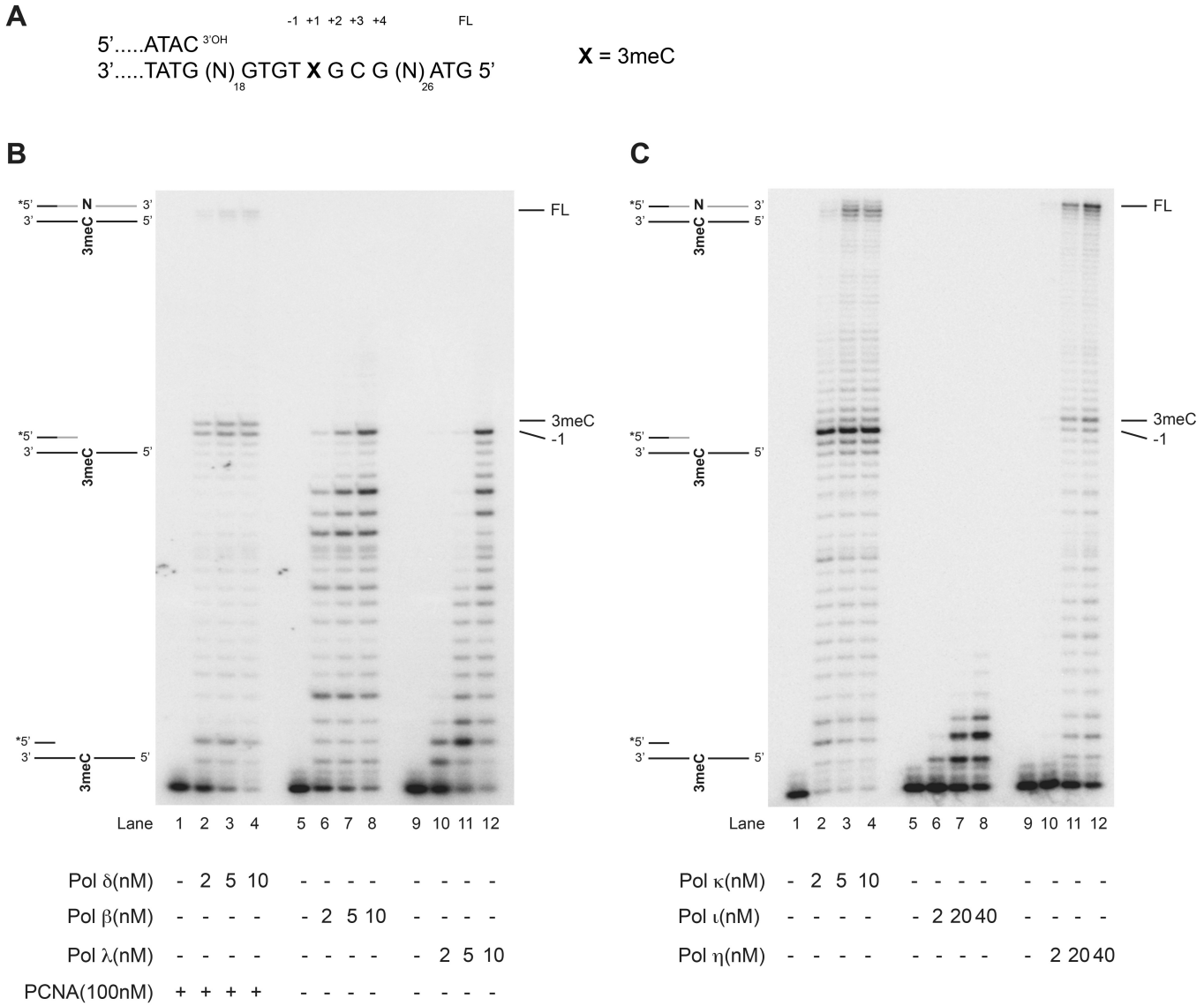

Figure 1. 3meC bypass by six human DNA polymerases under running-start conditions. (**A**) Schematic representation of running-start primer template containing 3meC lesion designated as X. Numbers above the template indicate the positions of template bases with respect to the lesion. FL stands for full-length. (**B**, **C**) Titration of Pols δ, β, λ (B) and Pols κ, ι, η (C) under running-start conditions in the presence of 2 nM DNA and indicated PCNA amounts. The experiments were done under conditions as described in 'Materials and Methods' section.

DNA polymerase η is the most proficient in filling 3meC containing DNA gaps, mimicking NER and BER intermediates

In addition to DNA replication, ssDNA regions frequently exist in the shape of gap intermediates produced during repair processes such as NER and BER. Generation of alkylation damage while the NER or BER machineries are still processing these ssDNA gaps would require lesion bypass for efficient gap closure. To determine the ability of Pols to close NER gap intermediate containing a lesion, a 29-nt gap construct with 3meC at position +23 was generated. As the presence of a phosphate group can dramatically affect bypass efficiency of certain Pols (29), the 5′-terminus of the gap was either phosphorylated (Figure 3A) or not (Supplementary Figure S3A). As expected, titration of Pol δ revealed that this Pol efficiently reached the 3meC, was able to incorporate a nucleotide opposite the lesion, but was poor in subsequent extension, resulting in inefficient gap filling independently of the gap 5′-end phosphorylation status (Figure 3B and Supplementary Figure S3B). While Pol β was once more blocked by 3meC, Pol λ, another X-family member, efficiently closed the 29-nt gap, when the 5′-end of the gap was phosphorylated, but not when the phosphate group was lacking (Figure 3B, lane 12 compare with Supplementary Figure S3B, lane 12). Interestingly, Pol λ predominately generated products one nucleotide shorter than the gap size (Figure 3B, lane 12), indicating that it either stops just before the 5′-end of the gap or it generates single

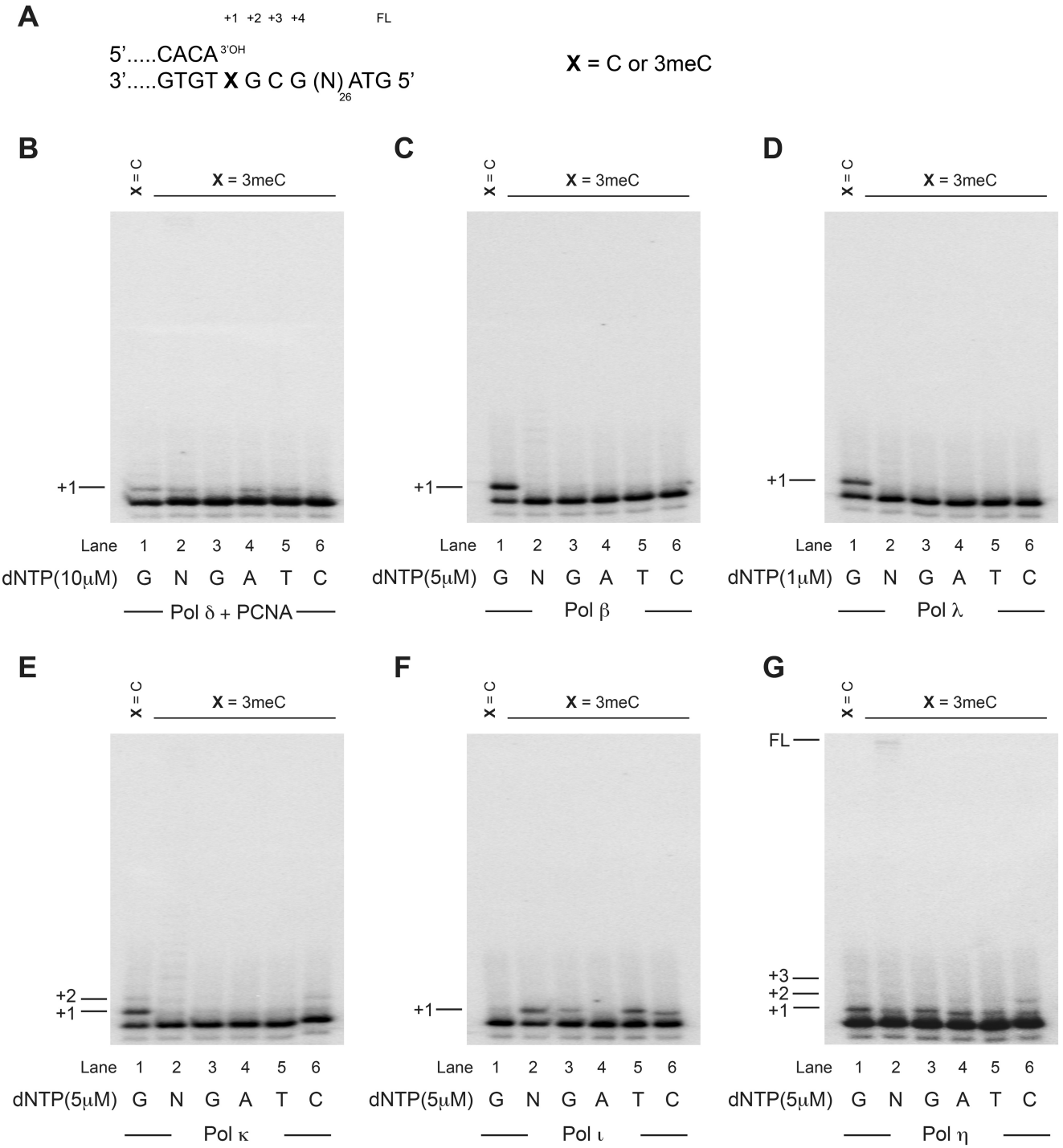

Figure 2. Efficiency and fidelity of six human DNA polymerases on the 3meC template under standing-start conditions. (**A**) Standing-start primer template with undamaged C or 3 meC lesion designated as X. Numbers above the template indicate the position of template bases with respect to the lesion at +1. FL is full-length product. (**B–G**) Extension of the 2 nM standing-start primer template by 2 nM Pol δ in the presence of 100 nM PCNA (B), 2 nM Pol β (C), 2 nM Pol λ (D), 2 nM Pol κ (E), 2 nM Pol ι (F) and 2 nM Pol η (G). Reactions in lanes 1 and 3–6 contain dGTP, dATP, dTTP and dCTP, respectively. In lane 2, all four dNTPs (N) were added. The experiments were performed under conditions as specified in 'Materials and Methods' section.

nucleotide deletions, potentially by looping out the lesion. Similarly to running start conditions, Pol ι was not able to reach the lesion (Figure 3C and Supplementary Figure S3C). Pol κ showed a strong pausing site immediately before the lesion but was eventually able to close the gap containing both non- and phosphorylated 5′-end (Figure 3C and Supplementary Figure S3C), as well as continuing up to the end of the template, displacing the downstream strand. Pol η on the other hand efficiently bypassed the lesion and completely filled the gap

Table 1. Kinetic parameters for nucleotide incorporation by DNA polymerases ι and η opposite 3meC in the template

	Pol ι				Pol η			
dNTP	k_M (μM)	k_{cat} (ms^{-1})	k_{cat}/k_M ($M^{-1}s^{-1}$)	Fidelity[a]	k_M (μM)	k_{cat} (ms^{-1})	k_{cat}/k_M ($M^{-1}s^{-1}$)	Fidelity[a]
dGTP	6	0.3	0.05×10^3		2	0.6	0.31×10^3	
dATP	n.a.	n.a.	n.a.	n.a.	1.5	0.7	0.46×10^3	0.7
dTTP	12.64	0.9	0.07×10^3	0.7	18.4	0.7	0.04×10^3	8.9
dCTP	3.5	0.2	0.05×10^3	0.9	2.4	0.3	0.14×10^3	2.2

Not accessible values designated as n.a.
[a]Calculated as $V_{max}/kM_{(dGTP)}/V_{max}/kM_{(d\ A/T/CTP)}$.
The experiments were done under conditions as specified in 'Materials and Methods' section.

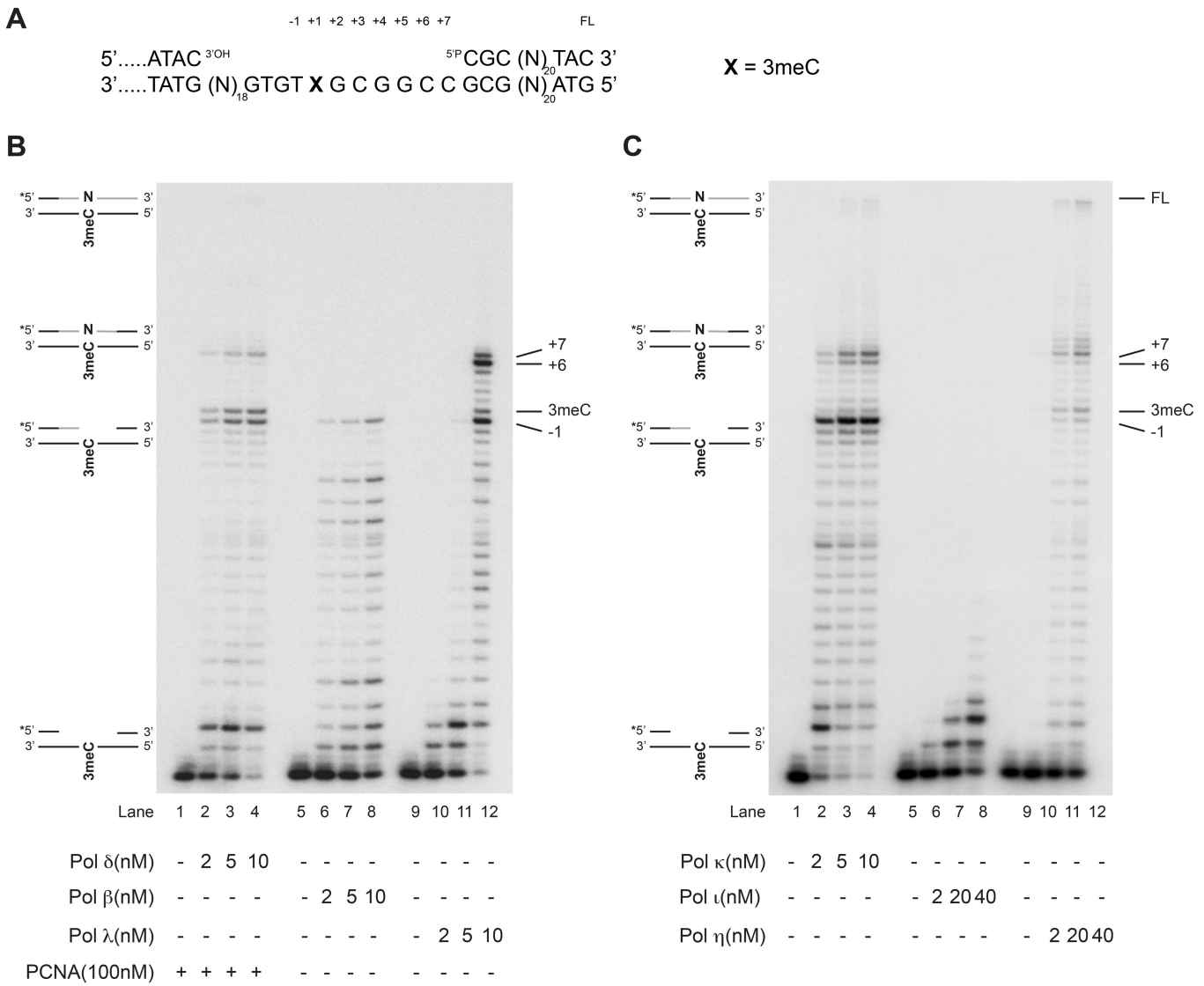

Figure 3. Synthesis by six human DNA polymerases past a 3meC lesion in the context of a NER intermediate. (**A**) Schematic representation of 29-nt gap template containing a 3meC lesion designated as X. Numbers indicate the position of template bases with respect to the lesion. FL stands for full-length product generated after strand displacement. (**B**, **C**) Titration of Pols δ, β, λ (B) and Pols κ, ι, η (C) in the presence of 2 nM DNA and indicated PCNA amounts. The experiments were done under conditions as described in 'Materials and Methods' section.

(Figure 3C and Supplementary Figure S3C). It also showed robust strand displacement of both phosphorylated and non-phosphorylated 5′-gap oligonucleotide (Figure 3C and Supplementary Figure S3C).

Next, the efficiency and accuracy of 3meC bypass were addressed on a shorter 7-nt gap template, mimicking a long-patch BER intermediate, with phosphorylated (Supplementary Figure S4A) or non-phosphorylated

(Supplementary Figure S5A) 5′-gap terminus and bearing the lesion at position +1. B-family Pol δ was impaired by 3meC lesion, irrespectively of the 5′-gap status and only weakly misincorporated dATP and dTTP, being then unable to continue synthesis (Supplementary Figures S4B and S5B). Even though Pol β is suited to fill short gaps, the presence of 3meC entirely blocked its activity (Supplementary Figures S4C and S5C). Pol κ was completely blocked with 5′-phosphorylated gap (Supplementary Figure S4E) and showed only a very weak activity on the unphosphorylated substrate (Supplementary Figure S5E). In contrast, Pol η again efficiently closed the gap, incorporating mainly the incorrect dATP and correct dGTP opposite the lesion, as well as to a lesser extent dCTP and dTTP (Supplementary Figures S4G and S5G). Pols λ and ι mispaired 3meC with dCTP (Supplementary Figure S4D, lane 6) and dTTP (Supplementary Figure S4F, lane 5 and Supplementary Figure S5F, lane 5), respectively. In comparison to standing-start conditions (Figure 2F), the presence of 3meC did not stimulate Pol ι activity. While Pol ι was unable to close the gap (Supplementary Figures S4F and S5F, lane 2), Pol λ after dCTP misincorporation reached the end of the gap, albeit with low efficiency and only when 5′ gap terminus was phosphorylated (compare Supplementary Figure S4D, lanes 2 and 6 to Supplementary Figure S5D, lanes 2 and 6). As under standing-start conditions Pol λ could not bypass 3meC (Figure 2D), the present observation raised the possibility that in the context of short-gap 3meC is not directly mispaired with dCTP, but instead that Pol λ uses its ability to scrunch the template (30) and loop out the lesion, thus incorporating dCTP opposite template G at position +1. However, it is also possible that the presence of the 5′-phosphate, which is known to increase the efficiency of Pol λ, may allow direct incorporation opposite the lesion.

DNA polymerases ι and η can fill a single-nucleotide gap positioned opposite 3meC

While long-patch BER is more common during replication, the majority of BER reactions in G1/G2 phases give raise to ssDNA in shape of a 1-nt gap intermediate, as a consequence of the combined glycosylase and AP endonuclease action. Thus, we next tested the fidelity on a template containing a 1-nt gap positioned opposite 3meC (Figure 4A) and bearing a 5′-phosphorylated end. Replicative Pol δ was as expected impaired at this template and extremely poorly misincorporated dATP and dTTP opposite the lesion (Figure 4B). Pol β was unable to act at the site of 3meC damage, even under these classical BER conditions (Figure 4C). Surprisingly, Pol λ that is known to efficiently perform TLS on 1-nt gap (26,31) was blocked in the presence of 3meC. This suggested that during copying of the larger 7- and 29-nt gaps (Figure 3 and Supplementary Figure S4) Pol λ scrunched the template, looped out the damaged nucleotide, elongated and consequently induced single nucleotide deletions. From the Y-family enzymes, Pol κ did not act on the lesion template (Figure 4E), whereas Pol ι and η efficiently filled the gap. Pol ι misincorporated dTTP (Figure 4F, lane 5) and its activity, similarly to 7-nt gap (Supplementary Figures S4 and S5), was not stimulated by 3meC. Thus, suggesting that presence of the lesion stimulates Pol ι activity only in replicative context (Figure 2F). Pol η on 1-nt gap template incorporated the correct dGTP, as well as the incorrect dATP (Figure 4G, lanes 3 and 4). Interestingly, on this template, no incorporation of dTTP or dCTP by Pol η was noted, contrary to what was observed under standing-start conditions and with the longer gaps. Further implying that the previously detected dCTP and dTTP incorporation by Pol η (Figures 2G, Supplementary Figure S4G and S5G), as well as dCTP by Pol κ (Figure 2E) resulted from incorporation opposite alternative templating bases, which cannot take place in a 1-nt gap. When all 4 dNTPs were present in the reaction Pol η generated a +1 product with electrophoretic mobility more similar to that of dATP than dGTP, indicating potentially inaccurate bypass of 3meC in a 1-nt gap (Figure 4G, compare lanes 2, 3 and 4). Taken together, as in the case of the previously used standing-start and gapped templates, Pols ι and η were the most proficient Pols in performing TLS over a 3meC lesions.

DNA polymerases κ and η are best extenders from 3meC

In many cases, TLS is a two-step process involving incorporation of a nucleotide opposite a lesion by a certain Pol and subsequent extension of the primer by a specialized extender Pol. To test the extension properties of different Pols, a primer/template ending with either the correct G:3meC or the three incorrect A:3meC, T:3meC or C:3meC base pairs was created (Figure 5A). All six tested human Pols successfully utilized the control C:G substrate, however with different efficiencies (Figure 5B, lanes 2–7). In presence of the lesion, Pol δ only weakly extended T:3meC and C:3meC containing constructs (Figure 5B, lanes 23 and 30). In contrast, Pols κ and η utilized both correctly, as well as all three incorrectly primed lesion templates (Figure 5B, lanes 12, 14, 19, 21, 26, 28, 33 and 35) and from all the six Pols tested were the two most efficient in extending all the substrates. While Pol η generated full-length products, Pol κ in contrary created products one or two nucleotides shorter than the full-length (Figure 5B, lanes 12,19, 26 and 33), in agreement with its tendency to introduce −1 deletions (32).

To address whether the observed extension capacity was construct dependent, we next generated a 6-nt gap with either correct G:3meC or incorrect A:3meC, T:3meC and C:3meC base pair located at the 3′-end of the gap (Supplementary Figure S6A). From these substrates, Pol δ only poorly processed A:3meC, C:3meC and T:3meC gaps (Supplementary Figure S6B, lanes 16, 23 and 30). Pol λ on the other hand was able to extend all lesion constructs and close 6-nt gap (Supplementary Figure S6B). Similarly, Pols κ and η acted on all the templates and, as with the previous substrates, were the most efficient extenders. Interestingly, under the 6-nt gap condition, Pol κ was the most active especially if gap contained T:3meC or C:3meC (Supplementary Figure S6B, lanes 26 and 33). Pol η, as well as Pol κ but only on the T:3meC substrate,

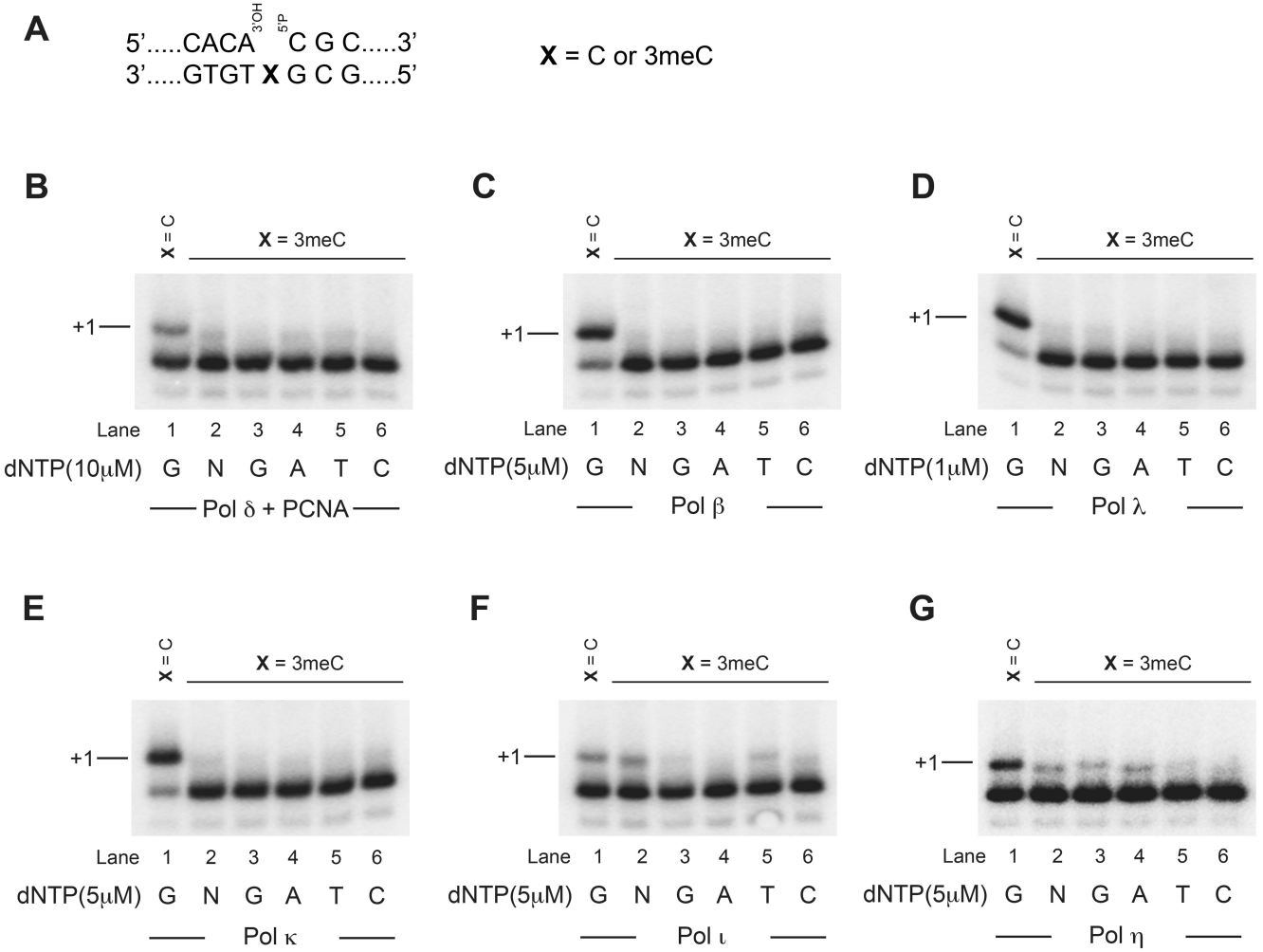

Figure 4. Ability of six human DNA polymerases to close a single nucleotide gap generated opposite a 3meC damage. (**A**) A 1-nt gap template with undamaged C or 3meC lesion (X) positioned directly opposite the gap. (**B–G**) Filling of the 2 nM gapped DNA template depicted in (A) by 2 nM Pol δ in the presence of 100 nM PCNA (B), 2 nM Pol β (C) 2 nM Pol λ (D), 2 nM Pol κ (E), 2 nM Pol ι (F) and 5 nM Pol η (G). Reactions in lanes 1 and 3–6 contain dGTP, dATP, dTTP and dCTP, respectively. In lane 2, all four dNTPs (N) were added. The experiments were done under conditions as specified in 'Materials and Methods' section.

displayed a robust strand displacement activity. In case of a C:3meC template, both Pols λ and κ predominantly generated five nucleotides long product, a patch one nucleotide shorter than the gap itself, thus indicating that both Pols potentially re-prime the template by repositioning the 3′ C and base-pairing it with G at position +1 from the lesion. In summary, these findings indicated that Pols κ and η are the most efficient extenders of 3meC, and that their activity is influenced by the structure of the DNA construct.

Efficient bypass of 3meC in human WCEs requires the presence of a functional DNA polymerase η

So far in the experiments testing recombinant human enzymes, we demonstrated that Pol ι successfully incorporated a nucleotide opposite 3meC, whereas Pol η was more efficient in extending a mismatched primer containing 3meC. Uniquely, among all Pols tested, Pol η was efficient in both: (i) incorporation opposite the lesion as well as (ii) subsequent extension (Figures 1–5). To verify whether Pol η was indeed playing a major role in 3meC bypass, even in the presence of other Pols such as in the context of a whole cell, we tested the fidelity and bypass capacity of various cellular extracts under standing-start conditions (Figure 6A). WCEs were prepared from XPV patient cells lacking endogenous functional Pol η. XPV cells were complemented with either (i) empty vector, (ii) human Pol η or (iii) Pol ι expression constructs (Figure 6B). Interestingly, although all three WCEs were comparably active on a control template containing undamaged C (Figure 6C, lanes 1, 7 and 13), only WCE prepared from XPV cells that had been complemented with Pol η showed robust incorporation opposite 3meC (Figure 6C, lanes 8–12). As with the recombinant enzyme (Figure 2G), Pol η complemented WCE predominantly incorporated dATP and dGTP opposite the 3meC (Figure 6C, lanes 9 and 10). In the presence of 4 dNTPs, +1 product with electrophoretic mobility similar to the one of A incorporated opposite the lesion was obtained

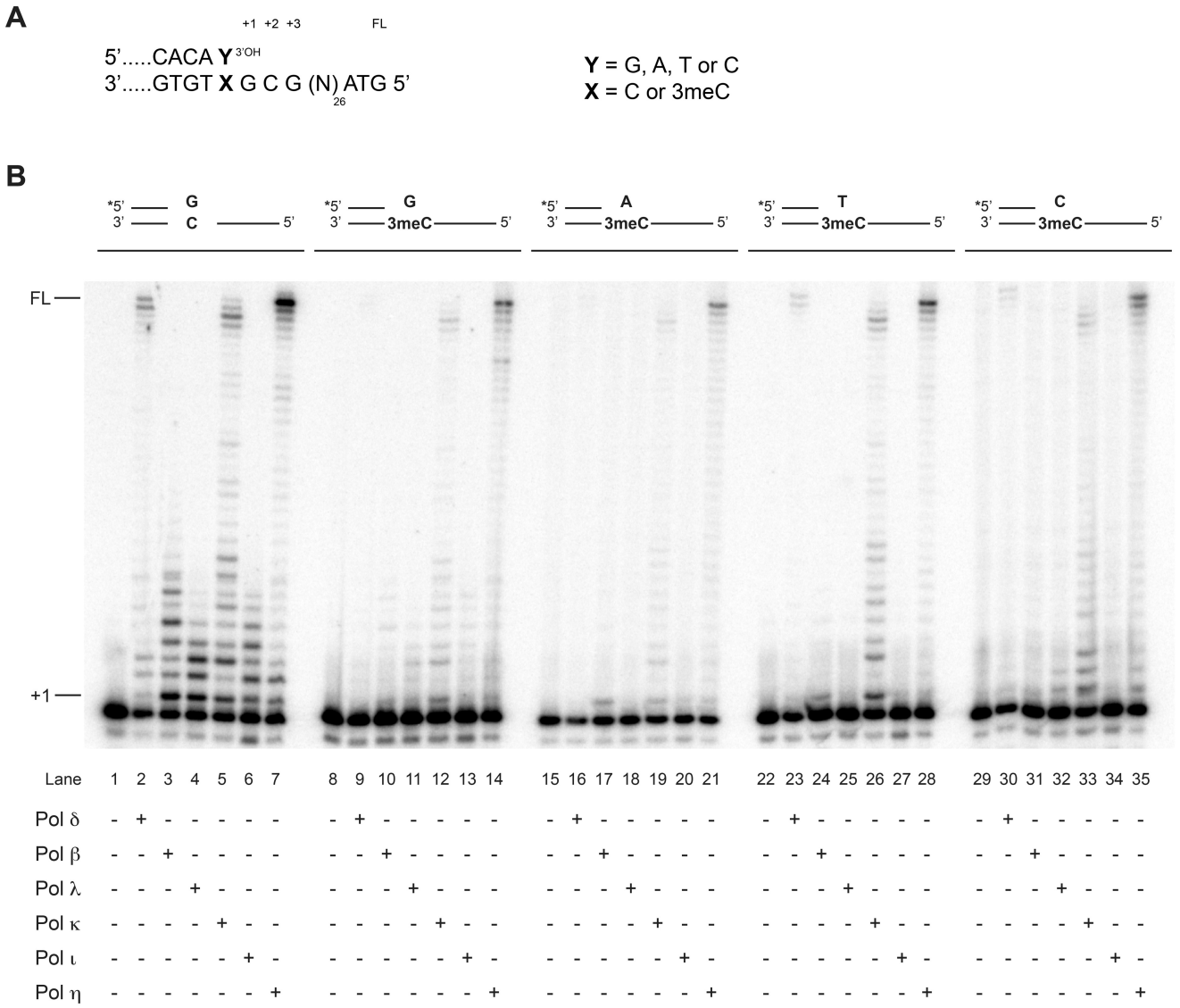

Figure 5. Extension of accurately base-paired and mispaired 3meC primer/templates by six human DNA polymerases. (**A**) Representation of incorrectly (Y = A, T or C) as well as correctly (Y = G) paired primer termini on control (X = C) and lesion (X = 3meC) DNA. Numbers above the template indicate the position of template bases with respect to the lesion at +1. (**B**) Extension of the 2 nM DNA template schematically represented above the lanes by 5 nM Pol δ in the presence of 100 nM PCNA, 4 nM Pol β, 7 nM Pol λ, 4 nM Pol κ, 30 nM Pol ι and 20 nM Pol η. The experiments were performed under conditions as described in 'Materials and Methods' section.

(Figure 6C, compare lanes 8 and 10). This suggested that Pol η potentially bypasses 3meC in an inaccurate manner and further coincided with the results of reactions using only the purified protein (Figure 4G). Pol η mediated bypass in context of WCE was partially efficient, due to low amount of extension product generated (Figure 6C, lane 8). We thus hypothesized that the simultaneous increase in the amounts of (i) Pol ι as inserter and (ii) Pol η as both inserter and extender of 3meC could improve the bypass efficiency. Expression of both Pols in XPV cells (Figure 6B) resulted in promoted incorporation of all 4 nucleotides (Figure 6C, lanes 21–24), as well as an increased amount of extension product (Figure 6C, compare lanes 8 and 20), overall leading to improved 3meC bypass efficiency. Taken together these findings clearly indicated that the presence of functional Pol η in human cells is crucial for 3meC bypass, which can be mediated by either Pol η alone or as a two-step process involving an additional Pol, such as Pol ι.

DISCUSSION

Exposure of genomic DNA to alkylating agents results in generation of numerous DNA lesions. While the pathways to repair alkylating DNA lesions are well characterized, much less is known about the influence of alkylation damage on different Pols. Several studies described the properties of prokaryotic Pols on the alkylation lesion 3meC; however, it is currently unknown how this damage affects eukaryotic Pols. In this work, we

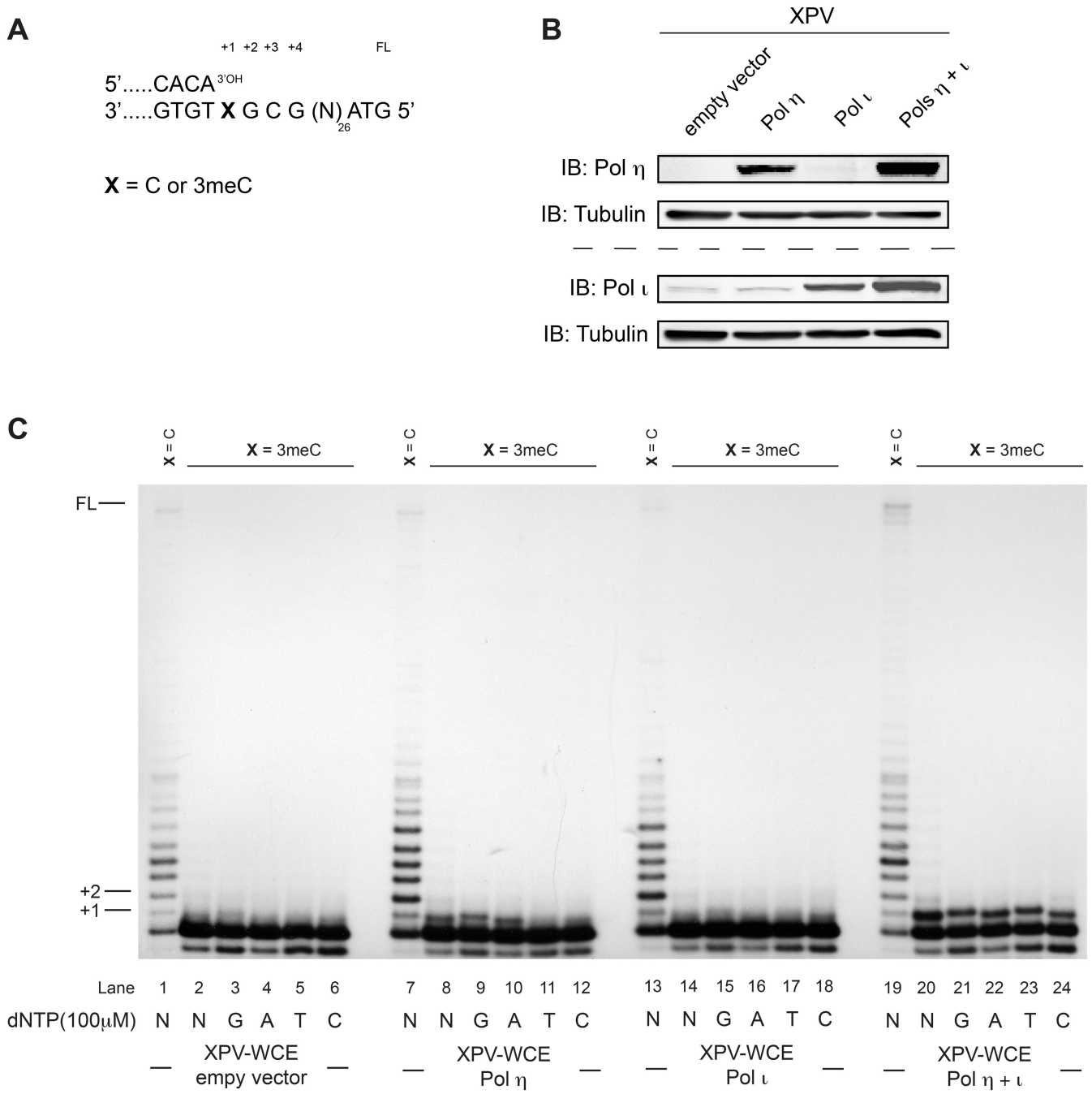

Figure 6. Only cells expressing DNA polymerase η are able to successfully overcome 3meC damage. (**A**) Schematic representation of standing-start primer template with undamaged C or 3meC lesion designated as X. Numbers above the template indicate the position of template bases with respect to the lesion at +1. FL is full-length product. (**B**) Immunoblot analysis of XPV WCE complemented with empty vector, Pol η, Pol ι or Pols η and ι expression vectors. (**C**) Bypass capacity of 3meC lesion by XPV, XPV Pol η, XPV Pol ι, as well as XPV Pols η and ι complemented extracts. The experiments were done under the conditions specified in 'Materials and Methods' section.

characterized the properties of 3meC bypass by the six human Pols δ, β, λ, κ, ι and η, members of the B-, X- and Y-families. Our findings strongly suggest that among the six tested enzymes, Polη most efficiently bypassed 3meC· On open or long gapped substrates, Pol η-mediated 3meC bypass was error-prone, leading to the incorporation of almost all four nucleotides with selectivity indexes ranging from 0.7 (for dATP) to 9 (for dTTP) with respect to the correct dGTP (Table 1). However, on single nucleotide gapped substrates, incorporation was restricted to dATP and dGTP (Figure 4G). Besides its ability to incorporate the incorrect dATP, as well as the correct dGTP opposite 3meC, Pol η efficiently extended both correctly and incorrectly paired primer termini on lesion DNA. Pol η was unique among all the tested Pols in combining the properties of both an inserter and

extender. We further confirmed its importance in the context of a whole cell; by showing that lack of Pol η in human cell extracts results in a severely reduced ability to act at the site of 3meC (Figure 6C). The importance of functional Pol η in response to monoalkylating agents has been already suggested by *in vivo* experiments showing that the *Saccharomyces cerevisiae* rad30D strain lacking Pol η is somewhat sensitive to MMS (33,34). Furthermore, MMS treatment of human cells was shown to result in formation of Pol η foci at the site of replication forks blocked by alkylation lesions (35), one of which is potentially 3meC. In addition to Pol η, another Y-family member, Pol ι efficiently bypassed 3meC by preferentially misincorporating dTTP opposite the lesion but was unable to extend it. In the context of WCEs, an increase in the level of Pol ι as inserter resulted in promoted Pol η-mediated 3meC bypass (Figure 6C). Interestingly, another Y-family enzyme, Pol κ, was a poor inserter but proved to be the most efficient in extending from a T:3meC mismatch. Although the generation of G:3meC pair by Pol η would create another chance for ALKBH2 to repair and thus remove lesion from the genome, it is currently not clear which consequences the persistence of A:3meC, as well as T:3meC, created by Pol η and ι respectively, would have on genome stability. If repair of A:3meC and T:3meC would be possible by ALKBH2 proteins, it would result in harmful mismatches and could potentially lead to mutations in the next round of DNA replication. Generation of mismatches would be especially detrimental in tissues lacking functional mismatch repair, as was observed for various tumour types (36,37). To prevent genomic instability in precancerous tissues, it would thus be crucial to activate a Pol that can rather faithful bypass 3meC, such as Pol η.

Under replicative conditions, 3meC impaired the activity of the B-family replicative Pol δ and blocked the repair Pols β and λ (Figure 1B). A similar finding was seen upon 3meC extension, condition under which Pol δ only very weakly generated full-length product. Thus suggesting that, upon encountering the lesion, the replication fork could potentially be stalled and for its successful continuation, another more specialized Pol, like Pol η, would be required. These results correlate well with findings obtained in prokaryotes demonstrating impeded activity of Pols I and III at the site of 3meC (10,18,19). Interestingly, though Pol λ was unable to directly incorporate nucleotides opposite the lesion, in the context of gapped DNA, larger than 1 nt, this Pol successfully scrunched the template and continued the synthesis by pairing the incoming nucleotide with the template base at +1 position from the lesion. The property of Pol λ to scrunch the template was directly shown by the crystal structure published previously by Garcia-Diaz *et al.* (30). Also, when the terminal nucleotide of the primer was complementary to the nucleotide immediately downstream the lesion, Pol λ was able to loop out 3meC and use the base downstream to re-align the primer. This slippage ability of Pol λ has been already observed for other lesions (38). In both cases, the result was a 1-nt deletion.

Based on our findings, we propose a model for 3meC bypass in context of DNA replication (Figure 7). When the lesion is not repaired by ALKBHs and remains present in the template strand, Pols might handle it in one of the following ways: (1) after copying 3meC by incorporating inaccurate dATP or dTTP, the replicative Pol δ is stalled, and TLS Pol η is recruited to extend the mispair (Figure 7-1); (2) the replication fork is stalled in front of 3meC leading to Pol η recruitment, predominant insertion of dATP opposite the lesion and the extension (Figure 7-2); (3) the replication fork is stalled in front of 3meC, Pol ι is recruited to tolerate the lesion by misincorporating dTTP and Pol η to extend the newly

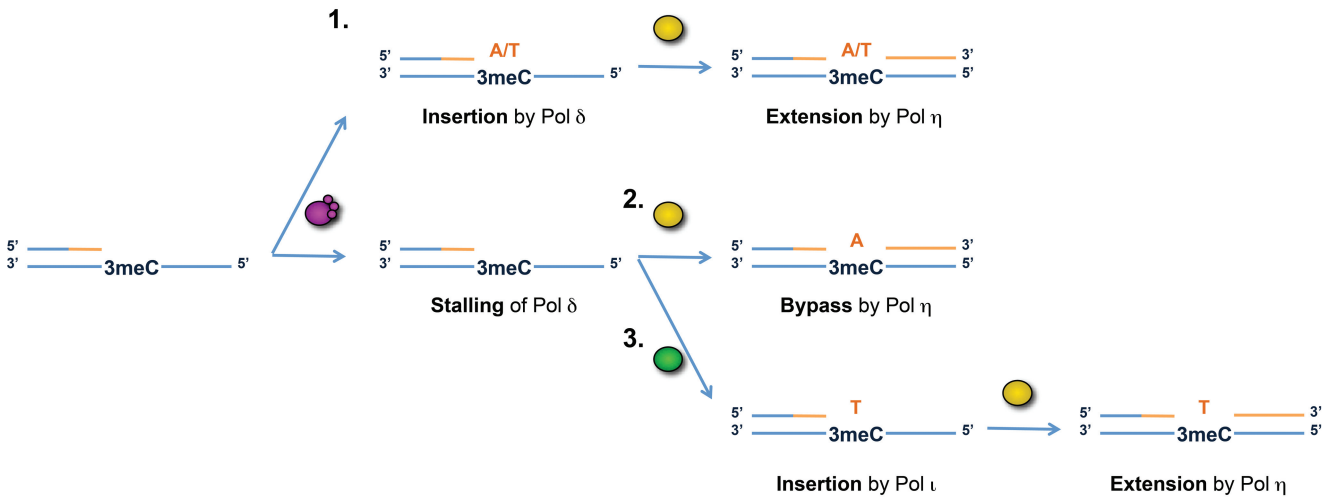

Figure 7. Model of 3meC bypass during DNA replication. If 3meC lesion (designated as X) is not repaired by ALKBHs and it remains present in the template strand, Pols might handle it in one of the following ways: (1) after copying 3meC, by predominantly incorporating inaccurate dATP or dTTP, replicative Pol δ is stalled and TLS Pol η is recruited to extend the mispair; (2) the replication fork is stalled in front of 3meC leading to Pol η recruitment, insertion of dATP opposite the lesion and the extension; (3) the replication fork is stalled in front of 3meC, Pol ι is recruited to tolerate the lesion by incorporating dTTP and Pol η to extend the newly formed T:3meC base-pair. For simplicity, only nucleotides preferentially incorporated by each of the Pols are depicted.

formed T:3meC base-pair (Figure 7-3). In summary, our findings suggest the potential existence of novel Pol η-dependent pathway that would enable cells to overcome cytotoxic effects of alkylating agents, even at the cost of potentially causing mutations, especially in the absence of functional direct reversal proteins.

SUPPLEMENTARY DATA

Supplementary Data are available at NAR Online.

ACKNOWLEDGEMENTS

The authors thank Ulrich Hübscher and Giovanni Maga for critical reading of the manuscript and their support. They are very grateful to researches for kindly sharing and providing the material: Roger Woodgate for Pol ι and η expression clones and Pol ι antibody; Allan Lehman for XP30R0 cells; as well as to Elena Ferrari for purifying Pol δ.

FUNDING

University of Zurich (to A.F. and B.v.L.). Funding for open access charge: University of Zurich.

Conflict of interest statement. None declared.

REFERENCES

1. Friedberg,E.C., Walker,G.C., Siede,W., Wood,R.D., Schultz,R.A. and Ellenburger,T. (2006) *DNA Repair and Mutagenesis*. ASM Press. Washington, DC, USA.
2. Fu,D., Calvo,J.A. and Samson,L.D. (2012) Balancing repair and tolerance of DNA damage caused by alkylating agents. *Nat. Rev. Cancer*, **12**, 104–120.
3. Sedgwick,B. (2004) Repairing DNA-methylation damage. *Nat. Rev. Mol. Cell Biol.*, **5**, 148–157.
4. Allan,J.M. and Travis,L.B. (2005) Mechanisms of therapy-related carcinogenesis. *Nat. Rev. Cancer*, **5**, 943–955.
5. Drablos,F., Feyzi,E., Aas,P.A., Vaagbo,C.B., Kavli,B., Bratlie,M.S., Pena-Diaz,J., Otterlei,M., Slupphaug,G. and Krokan,H.E. (2004) Alkylation damage in DNA and RNA—repair mechanisms and medical significance. *DNA Repair (Amst.)*, **3**, 1389–1407.
6. Bodell,W.J. and Singer,B. (1979) Influence of hydrogen bonding in DNA and polynucleotides on reaction of nitrogens and oxygens toward ethylnitrosourea. *Biochemistry*, **18**, 2860–2863.
7. Trewick,S.C., Henshaw,T.F., Hausinger,R.P., Lindahl,T. and Sedgwick,B. (2002) Oxidative demethylation by *Escherichia coli* AlkB directly reverts DNA base damage. *Nature*, **419**, 174–178.
8. Duncan,T., Trewick,S.C., Koivisto,P., Bates,P.A., Lindahl,T. and Sedgwick,B. (2002) Reversal of DNA alkylation damage by two human dioxygenases. *Proc. Natl Acad. Sci. USA*, **99**, 16660–16665.
9. Aas,P.A., Otterlei,M., Falnes,P.O., Vagbo,C.B., Skorpen,F., Akbari,M., Sundheim,O., Bjoras,M., Slupphaug,G., Seeberg,E. *et al.* (2003) Human and bacterial oxidative demethylases repair alkylation damage in both RNA and DNA. *Nature*, **421**, 859–863.
10. Delaney,J.C. and Essigmann,J.M. (2004) Mutagenesis, genotoxicity, and repair of 1-methyladenine, 3-alkylcytosines, 1-methylguanine, and 3-methylthymine in alkB *Escherichia coli*. *Proc. Natl Acad. Sci. USA*, **101**, 14051–14056.
11. Sikora,A., Mielecki,D., Chojnacka,A., Nieminuszczy,J., Wrzesinski,M. and Grzesiuk,E. (2010) Lethal and mutagenic properties of MMS-generated DNA lesions in *Escherichia coli* cells deficient in BER and AlkB-directed DNA repair. *Mutagenesis*, **25**, 139–147.
12. Ringvoll,J., Nordstrand,L.M., Vagbo,C.B., Talstad,V., Reite,K., Aas,P.A., Lauritzen,K.H., Liabakk,N.B., Bjork,A., Doughty,R.W. *et al.* (2006) Repair deficient mice reveal mABH2 as the primary oxidative demethylase for repairing 1meA and 3meC lesions in DNA. *EMBO J.*, **25**, 2189–2198.
13. Nay,S.L., Lee,D.H., Bates,S.E. and O'Connor,T.R. (2012) Alkbh2 protects against lethality and mutation in primary mouse embryonic fibroblasts. *DNA Repair (Amst.)*, **11**, 502–510.
14. Wu,S.S., Xu,W., Liu,S., Chen,B., Wang,X.L., Wang,Y., Liu,S.F. and Wu,J.Q. (2011) Down-regulation of ALKBH2 increases cisplatin sensitivity in H1299 lung cancer cells. *Acta Pharmacol. Sin.*, **32**, 393–398.
15. Fujii,T., Shimada,K., Anai,S., Fujimoto,K. and Konishi,N. (2013) ALKBH2, a novel AlkB homologue, contributes to human bladder cancer progression by regulating MUC1 expression. *Cancer Sci.*, **104**, 321–327.
16. Goodman,M.F. (2002) Error-prone repair DNA polymerases in prokaryotes and eukaryotes. *Annu. Rev. Biochem.*, **71**, 17–50.
17. Hubscher,U., Spadari,S., Villani,G. and Maga,G. (2010) *DNA Polymerases: Discovery, Characterization and Functions in Cellular DNA Transactions*. World Scientific Co. Pte. Ltd, New Jersey.
18. Boiteux,S. and Laval,J. (1982) Mutagenesis by alkylating agents: coding properties for DNA polymerase of poly (dC) template containing 3-methylcytosine. *Biochimie*, **64**, 637–641.
19. Saffhill,R. (1984) Differences in the promutagenic nature of 3-methylcytosine as revealed by DNA and RNA polymerising enzymes. *Carcinogenesis*, **5**, 691–693.
20. Hubscher,U. and Maga,G. (2011) DNA replication and repair bypass machines. *Curr. Opin. Chem. Biol.*, **15**, 627–635.
21. Lange,S.S., Takata,K. and Wood,R.D. (2011) DNA polymerases and cancer. *Nat. Rev. Cancer*, **11**, 96–110.
22. Yang,W. and Woodgate,R. (2007) What a difference a decade makes: insights into translesion DNA synthesis. *Proc. Natl Acad. Sci. USA*, **104**, 15591–15598.
23. Rechkoblit,O., Delaney,J.C., Essigmann,J.M. and Patel,D.J. (2011) Implications for damage recognition during Dpo4-mediated mutagenic bypass of m1G and m3C lesions. *Structure*, **19**, 821–832.
24. Jonsson,Z.O., Hindges,R. and Hubscher,U. (1998) Regulation of DNA replication and repair proteins through interaction with the front side of proliferating cell nuclear antigen. *EMBO J.*, **17**, 2412–2425.
25. Podust,V.N., Chang,L.S., Ott,R., Dianov,G.L. and Fanning,E. (2002) Reconstitution of human DNA polymerase delta using recombinant baculoviruses: the p12 subunit potentiates DNA polymerizing activity of the four-subunit enzyme. *J. Biol. Chem.*, **277**, 3894–3901.
26. van Loon,B. and Hubscher,U. (2009) An 8-oxo-guanine repair pathway coordinated by MUTYH glycosylase and DNA polymerase lambda. *Proc. Natl Acad. Sci. USA*, **106**, 18201–18206.
27. Frank,E.G., McDonald,J.P., Karata,K., Huston,D. and Woodgate,R. (2012) A strategy for the expression of recombinant proteins traditionally hard to purify. *Anal Biochem.*, **429**, 132–139.
28. Tissier,A., McDonald,J.P., Frank,E.G. and Woodgate,R. (2000) poliota, a remarkably error-prone human DNA polymerase. *Genes Dev.*, **14**, 1642–1650.
29. Villani,G., Hubscher,U., Gironis,N., Parkkinen,S., Pospiech,H., Shevelev,I., di Cicco,G., Markkanen,E., Syvaoja,J.E. and Tanguy Le Gac,N. (2011) *In vitro* gap-directed translesion DNA synthesis of an abasic site involving human DNA polymerases epsilon, lambda, and beta. *J. Biol. Chem.*, **286**, 32094–32104.
30. Garcia-Diaz,M., Bebenek,K., Larrea,A.A., Havener,J.M., Perera,L., Krahn,J.M., Pedersen,L.C., Ramsden,D.A. and Kunkel,T.A. (2009) Template strand scrunching during DNA gap repair synthesis by human polymerase lambda. *Nat. Struct. Mol. Biol.*, **16**, 967–972.
31. Maga,G., Crespan,E., Wimmer,U., van Loon,B., Amoroso,A., Mondello,C., Belgiovine,C., Ferrari,E., Locatelli,G., Villani,G. *et al.* (2008) Replication protein A and proliferating cell nuclear

antigen coordinate DNA polymerase selection in 8-oxo-guanine repair. *Proc. Natl Acad. Sci. USA*, **105**, 20689–20694.
32. Mukherjee,P., Lahiri,I. and Pata,J.D. (2013) Human polymerase kappa uses a template-slippage deletion mechanism, but can realign the slipped strands to favour base substitution mutations over deletions. *Nucleic Acids Res.*, **41**, 5024–5035.
33. Roush,A.A., Suarez,M., Friedberg,E.C., Radman,M. and Siede,W. (1998) Deletion of the Saccharomyces cerevisiae gene RAD30 encoding an *Escherichia coli* DinB homolog confers UV radiation sensitivity and altered mutability. *Mol. Gen. Genet.*, **257**, 686–692.
34. Begley,T.J., Rosenbach,A.S., Ideker,T. and Samson,L.D. (2002) Damage recovery pathways in *Saccharomyces cerevisiae* revealed by genomic phenotyping and interactome mapping. *Mol. Cancer Res.*, **1**, 103–112.
35. Kannouche,P., Broughton,B.C., Volker,M., Hanaoka,F., Mullenders,L.H. and Lehmann,A.R. (2001) Domain structure, localization, and function of DNA polymerase eta, defective in xeroderma pigmentosum variant cells. *Genes Dev.*, **15**, 158–172.
36. Marra,G. and Jiricny,J. (2005) DNA mismatch repair and colon cancer. *Adv. Exp. Med. Biol.*, **570**, 85–123.
37. Poulogiannis,G., Frayling,I.M. and Arends,M.J. (2010) DNA mismatch repair deficiency in sporadic colorectal cancer and Lynch syndrome. *Histopathology*, **56**, 167–179.
38. Blanca,G., Villani,G., Shevelev,I., Ramadan,K., Spadari,S., Hubscher,U. and Maga,G. (2004) Human DNA polymerases lambda and beta show different efficiencies of translesion DNA synthesis past abasic sites and alternative mechanisms for frameshift generation. *Biochemistry*, **43**, 11605–11615.